Synthesis and Spectroscopic Properties of Di-2-pyridyl Sulfide (dps) Compounds. Crystal Structure of $[Ru(dps)_2Cl_2]$†

Giuseppe Bruno, Franco Nicolò, Sanda Lo Schiavo, Maria S. Sinicropi and Giuseppe Tresoldi*
Dipartimento di Chimica Inorganica Analitica e Struttura Molecolare, Università di Messina,
Villaggio S. Agata, 98166 Messina, Italy

Bis(di-2-pyridyl sulfide)ruthenium(II) complexes containing the ligands Cl, NO_2, NO, MeCN, py (pyridine), pyz (pyrazine) or 4,4′-bipy (4,4′-bipyridine) have been prepared by usual methods and a new direct procedure from robust $[Ru(dps)_2Cl_2]$ **1a** (dps = di-2-pyridyl sulfide). This is the main product of the reaction between dps and $RuCl_3$ in refluxing dimethylformamide (dmf) while minor products are the complexes $[Ru(dps)(dmf)(CO)Cl_2]$ and $[Ru(dps)_2(CO)Cl][PF_6]$. The crystal structure of **1a** has been determined: orthorhombic, space group *Pbcn*, $a = 8.587(2)$, $b = 16.421(3)$, $c = 15.023(3)$ Å, $Z = 4$ and $R = 0.024$. The Ru atom exhibits an almost ideal octahedral co-ordination geometry involving two Cl atoms, in *cis* position, and the two dps ligands chelated through the respective pyridine N atoms. Each dps adopts a twisted N,N-inside conformation. The six-membered chelate rings show boat conformations with the Ru and S atoms out of the plane through the other four atoms on the same side. Oxidation of **1a** by HNO_3 or cerium(IV) salts, followed by precipitation with NH_4PF_6, gave $[Ru(dps)_2Cl_2][PF_6]$. The complexes have been characterized by infrared, UV/VIS, ^1H and ^{13}C NMR spectroscopies. The ^1H NMR resonances of the pyz and 4,4′-bipy derivatives were assigned by employment of correlation spectra. The lowest-energy band in the visible spectrum of **1a**, assigned as a $d_\pi(Ru) \longrightarrow \pi^*(dps)$ transition, is blue shifted with respect to that of $[Ru(2,2'\text{-bipy})_2Cl_2]$. Further blue shifts are observed on replacing in the Cl^- **1a** by stronger π-acceptor ligands such as NO_2^-, MeCN and NO^+.

The chemistry of mono- and di-nuclear ruthenium compounds containing bipyridine or polypyridine ligands has recently been reported extensively.[1–9] This interest has stemmed mainly from the relevance of this chemistry to photophysical, photochemical and redox phenomena.[2–8]

Mononuclear ruthenium(II) complexes of the type *cis*-$[Ru(bipy)_2X(X')]$ (bipy = 2,2′-bipyridine or related ligands, X and X′ = ancillary ligands) are of great importance because of their potential application as catalysts for the photodecomposition of water.[3,4] Important aspects of the co-ordination chemistry of the polypyridines towards ruthenium(II) substrates are the stereochemistry of the reaction products,[4,5] and the nature of the chelating and ancillary ligands which influence the excited-state and the redox properties of these complexes.[6]

On the other hand, binuclear ruthenium complexes have attracted much attention due to their ability to transfer two electrons[7] as well as to yield mixed-valence complexes that are of fundamental interest in the electron-transfer field.[8] The physical properties of the latters have been studied in the light of the Hush model with particular regard to the position, shape and intensity of the intervalence transition which yield information about the interaction between the metal centres.

Despite the large body of work devoted to the synthesis and characterization of binuclear ruthenium(II) complexes containing bipy as chelating ligand little attention has been focused on the incorporation of non-planar chelating ligands in the co-ordination sphere of ruthenium and most of the complexes examined are of the general type $[L_2Ru(L\text{–}L)RuL_2]^{4+}$ [L = bipy or bipy-like ligand; L–L = 2,3-bis(2-pyridyl)pyrazine, 2,2′-bipyrimidine, 'back-to-back' bis(bipyridine) or bis(terpyridine)]. Although unusual synthetic routes were recently reported,[9] these complexes are easily prepared by treating $[RuL_2Cl_2]$ with L–L in refluxing aqueous ethanol. On replacing bipy with non-planar chelating ligands these synthetic routes fail very likely for steric reasons.[1b,4] On the other hand the methods[8a,b,10] used to prepare binuclear complexes containing exobidentate bridging ligands of general type $[L_2XRu(L\text{–}L)RuXL_2]^{2+}$ (X = Cl or NO_2; L–L = pyrazine or 4,4′-bipyridine) are lengthy (L = planar chelating ligand) or inefficient (L = non-planar chelating ligand) because they involve $[RuL_2X(solvent)]^+$ species which are inert to substitution or too labile.

Following our interest in the chemistry of the bipyridine-like compound di-2-pyridyl sulfide (dps)[11] we were particularly interested to know how it would modify the physical properties of the ruthenium complexes. In this work, as a preliminary step towards the synthesis of mixed-valence species which is the long-term goal of our work, we focus attention on the synthesis and characterization of ruthenium(II) complexes containing dps as a polypyridine ligand. We have developed a relatively simple synthetic method which allows to prepare mono- or bi-nuclear complexes containing dibasic ligands such as pyrazine (pyz) or 4,4′-bipy from robust $[Ru(dps)_2Cl_2]$ and silver salts (ratio 1 : 1). The crystal structure of the precursor $[Ru(dps)_2Cl_2]$ is also reported.

Experimental

Di-2-pyridyl sulfide[12] and $[Ru(2,2'\text{-bipy})Cl_2]$[1a] were prepared by published methods. Elemental analyses were carried by Redox Microanalytical Laboratory of Cologno Monzese (Milano). Conductivity measurements were done on a Radiometer CDM 3 conductivity meter. Infrared spectra were recorded on a FT-IR 1720X spectrophotometer with samples as

---

New Ruthenium Complexes containing Polypyridine Ligands. Part 1.

† *Supplementary data available:* see Instructions for Authors, *J. Chem. Soc., Dalton Trans.*, 1995, Issue 1, pp. xxv–xxx.

Nujol mulls placed between CsI plates, electronic absorption spectra on a Perkin-Elmer Lambda 5 spectrophotometer and ^{1}H and ^{13}C NMR spectra on a Bruker AMX 300 spectrometer. All the products were dried over P_4O_{10} *in vacuo*. Crystallization, unless stated otherwise, was performed by dissolving the product in acetone and filtering into an excess of stirred diethyl ether. The synthesis and working up of the binuclear species were performed as far as possible in the dark.

Preparations.—$[Ru(dps)_2Cl_2]\cdot 2H_2O$ **1a**. The compounds $RuCl_3\cdot 3H_2O$ (1 g, 3.8 mmol), LiCl (1 g, 23.6 mmol) and dps (1.5 g, 8.0 mmol) were refluxed in dimethylformamide (dmf) (20 cm^3) under N_2 for 4 h. After cooling at room temperature and addition of acetone (50 cm^3) the mixture was allowed to stand at 0 °C overnight, giving a red solid which was filtered off, washed with acetone (until the filtrate was colourless) and copiously with water, then dried overnight and washed again three times with chloroform–acetone (1:2). Yield: 1.5 g (68%) (Found: C, 41.20; H, 3.50; N, 9.50; S, 10.90. $C_{20}H_{20}Cl_2N_4O_2RuS_2$ requires C, 41.10; H, 3.45; N, 9.60; S, 10.95%). IR: 1585s, 1578s, 1552s, 1545s, 781vs, 772vs, 760vs, 744vs, 303ms and 297ms cm^{-1}.

$[Ru(dps)(dmf)(CO)Cl_2]\cdot 2H_2O$ **2**. To the acetone–chloroform washes from the above preparation was added diethyl ether (120 cm^3) and the mixture was cooled overnight at −15 °C. The orange solid obtained was filtered off, washed with acetone (30 cm^3), diethyl ether (copiously) and crystallized from $CHCl_3$–hexane. Yield: *ca.* 10% (Found: C, 33.70; H, 3.80; N, 8.60; S, 6.35. $C_{14}H_{19}Cl_2N_3O_4RuS$ requires C, 33.80; H, 3.85; N, 8.45; S, 6.45%). IR: 1943vs, 1587s, 1553s, 824s, 769vs, 306s and 296s cm^{-1}. NMR (solvent $CDCl_3$, 298 K, standard $SiMe_4$): ^{1}H (300 MHz), δ 9.59 (2 H, m, 2H^6), 8.38 (1 H, br, HCO), 7.64 (4 H, m, 2H^4, 2H^3), 7.27 (2 H, m, 2H^5), 2.83 (3 H, s, CH_3) and 1.60 (3 H, s, CH_3); ^{13}C (75.56 MHz), δ 159.64 (C^6), 155.15 (C^2), 137.24 (C^4), 126.16 (C^3), 123.69 (C^5), 36.07 (CH_3) and 30.93 (CH_3).

$[Ru(dps)_2(CO)Cl][PF_6]$ **3**. The acetone washes from the above preparation were added to water (150 cm^3) containing an excess of NH_4PF_6. The yellow precipitate obtained was washed copiously with water, dried and crystallized twice. Yield *ca.* 10% (Found: C, 36.80; H, 2.40; N, 8.10; S, 9.20. $C_{21}H_{16}ClF_6N_4OPRuS_2$ requires C, 36.75; H, 2.35; N, 8.15; S, 9.35%). IR: 1972vs, 1590s, 1542s, 845vs, 767s, 559s and 307 ms cm^{-1}. Λ_M(MeCN, 2×10^{-4} mol dm^{-3}, 20 °C) = 160 Ω^{-1} cm^2 mol^{-1}. NMR ($CDCl_3$, 298 K, $SiMe_4$): ^{1}H (300 MHz), δ 9.5 (2 H, m, 2H^6), 8.49 (2 H, m, 2H^6), 7.60 (6 H, m, 4H^4, 2H^3), 7.50 (2 H, m, 2H^3), 7.37 (2 H, m, 2H^5) and 7.31 (2 H, m, 2H^5); ^{13}C (75.56 MHz), δ 161.73 and 159.64 (C^6), 135.39 and 134.11 (C^4), 126.29 and 125.66 (C^3), 123.14 and 123.01 (C^5).

$[Ru(dps)_2(NO_2)_2]\cdot H_2O$ **1b**. The complex $[Ru(dps)_2Cl_2]\cdot 2H_2O$ (0.585 g, 1 mmol) was refluxed for 1 h in water (150 cm^3). The yellow solution of the aqua species was filtered and the red residue refluxed again in water (100 cm^3). This procedure was repeated until the red residue was dissolved almost completely. The solution was concentrated to 100 cm^3 and then $NaNO_2$ (0.14 g, 2 mmol) was added. The orange solid obtained was washed with water. Yield: 0.41 g, (70%) (Found: C, 41.00; H, 3.00; N, 14.30; S, 11.00. $C_{20}H_{18}N_6O_5RuS_2$ requires C, 40.90; H, 3.10; N, 14.30; S, 10.90%). IR: 1588vs, 1551s, 1340vs, 1320vs, 1302vs, 1288vs, 820vs, 786vs, 779vs, 727s and 531s cm^{-1}.

$[Ru(dps)_2(MeCN)_2][PF_6]_2$ **1c**. The complex $[Ru(dps)_2Cl_2]\cdot 2H_2O$ (0.293 g, 0.5 mmol) and $AgPF_6$ (0.252 g, 1 mmol) were mixed in MeCN (25 cm^3) and stirred for 1 d in the dark. The yellow solution obtained was filtered into diethyl ether (100 cm^3) to precipitate a crude product which was crystallized twice. Yield 0.3 g (70%) (Found: C, 34.05; H, 2.55; N, 9.95; S, 7.50. $C_{24}H_{22}F_{12}N_6P_2RuS_2$ requires C, 33.95; H, 2.60; N, 9.90; S, 7.55%). IR: 2061 (br), 2040 (br), 1951s, 1559s, 1554s, 872vs, 840vs, 771vs and 558s cm^{-1} Λ_M(MeCN, 2×10^{-4} mol dm^{-3}, 20 °C) = 310 Ω^{-1} cm^2 mol^{-1}.

$[Ru(bipy)_2(dps)][PF_6]_2$ **4**. The complex $[Ru(bipy)Cl_2]$ (0.484 g, 1 mmol) and dps (0.226 g, 1.2 mmol) were refluxed in ethanol (15 cm^3) for 2 h under N_2. The yellow solution obtained was filtered and added to a stirred aqueous solution (50 cm^3) of NH_4PF_6 (1.63 g, 10 mmol). The crude product obtained was collected, washed copiously with water, dried overnight and crystallized. Yield 0.7 g (77%) (Found: C, 40.60; H, 2.80; N, 9.30; S, 3.50. $C_{30}H_{24}F_{12}N_6P_2RuS$ requires C, 40.40; H, 2.70; N, 9.45; S, 3.60%). IR: 1604s, 1588ms, 842vs, 762s, 741ms and 558vs cm^{-1}. Λ_M(MeCN, 2×10^{-4} mol dm^{-3}, 20 °C) = 305 Ω^{-1} cm^2 mol^{-1}.

$[Ru(dps)_2(NO)Cl][PF_6]_2$ **5a**. The complex $[Ru(dps)_2Cl_2]\cdot 2H_2O$ (0.585 g, 1 mmol) was dissolved in water as described for **1b**. To a stirred solution (50 cm^3) of the aqua species were added 1 mol dm^{-3} HCl (5 cm^3) and dropwise 10 cm^3 of a solution containing $NaNO_2$ (69 mg, 1.00 mmol). After complete addition the solution was warmed at 50 °C for 20 min. A saturated solution of NH_4PF_6 in water was added dropwise until a yellow precipitate formed. The stirred solution was cooled at room temperature and the solid filtered off and washed copiously with water. The product was crystallized twice. Yield: 0.58 g (70%) (Found: C, 28.80; H, 2.05; N, 8.50; S, 7.60. $C_{20}H_{16}ClF_{12}N_5OP_2RuS_2$ requires C, 28.85; H, 1.95; N, 8.40; S, 7.70%). IR: 1921vs, 1595s, 1567ms, 840 (br), 770s, 734ms, 558vs and 330ms cm^{-1}. Λ_M(MeCN, 2×10^{-4} mol dm^{-3}, 20 °C) = 301 Ω^{-1} cm^2 mol^{-1}.

$[Ru(dps)_2(NO)(NO_2)][PF_6]_2\cdot H_2O$ **5b**. The complex $[Ru(dps)_2(NO_2)_2]\cdot H_2O$ (0.588 g, 1 mmol) was suspended in methanol (50 cm^3) with stirring. A 70% aqueous solution of HPF_6 (5 cm^3) was added dropwise. The suspension was stirred for 1 h, filtered, washed with methanol (three times) and diethyl ether and crystallized. Yield: 0.73 g (85%) (Found: C, 28.00; H, 2.05; N, 9.70; S, 7.40. $C_{20}H_{18}F_{12}N_6O_4P_2RuS_2$ requires C, 27.90; H, 2.10; N, 9.75; S, 7.45%). IR: 1932vs, 1594vs, 1564ms, 1437vs, 1315vs, 842 (br), 782s, 736s and 558vs cm^{-1}. Λ_M(MeCN, 2×10^{-4} mol dm^{-3}, 20 °C) = 310 Ω^{-1} cm^2 mol^{-1}.

$[Ru(dps)_2(pyz)X][PF_6]\cdot nH_2O$ (X = Cl, n = 1 **6a**; X = NO_2, n = 2 **6b**). Potassium azide (0.040g, 0.5 mmol) was dissolved in warm methanol (10 cm^3) and added dropwise to a solution of $[Ru(dps)_2(NO)X][PF_6]_2$ (0.5 mmol) in acetone (30 cm^3). The dark red solution obtained was stirred for 20 min and filtered into an acetone solution (20 cm^3) containing a ten-fold excess of pyrazine (0.40 g, 5.0 mmol). The solution was warmed at 40 °C for 1 h with stirring and then anhydrous ether was added until complete precipitation of an orange solid. The solid was filtered off, washed copiously with diethyl ether and crystallized twice. Yield: 60% for both complexes: **6a** (Found: C, 38.05; H, 2.95; N, 11.10; S, 8.55. $C_{24}H_{22}ClF_6N_6ORuS_2$ requires C, 38.15; H, 2.95; H, 11.10; S, 8.50%). IR: 1589s, 1553ms, 840 (br), 770s, 726ms, 559vs and 232m cm^{-1} Λ_M(MeCN, 2×10^{-4} mol dm^{-3}, 20 °C) = 170 Ω^{-1} cm^2 mol^{-1}; **6b** (Found: C, 36.65; H, 3.05; N, 12.25; S, 8.05. $C_{24}H_{24}F_6N_7O_4PRuS_2$ requires C, 36.75; H, 3.10; N, 12.50; S, 8.15%). IR: 1588s, 1554ms, 1336s, 834 (br), 769s, 727ms and 559vs cm^{-1}. Λ_M(MeCN, 2×10^{-4} mol dm^{-3}, 20 °C) = 165 Ω^{-1} cm^2 mol^{-1}.

$[\{Ru(dps)_2Cl\}_2(\mu\text{-pyz})][PF_6]_2\cdot 2H_2O$ **7a** *and* $[\{Ru(dps)_2(NO_2)\}_2(\mu\text{-pyz})][PF_6]_2\cdot 0.5Me_2CO$ **7b**. These binuclear complexes were first prepared by the known routes.

(1) Potassium azide (0.040 g, 0.5 mmol) was dissolved in warm methanol (7 cm^3) and added dropwise to a solution of $[Ru(dps)_2(NO)X][PF_6]_2$ (0.5 mmol) in acetone (10 cm^3). The dark red solution obtained was stirred for 20 min and filtered into an acetone solution (5 cm^3) containing pyrazine (0.020g, 0.25 mmol). The solution was protected from light and stirred under N_2 for 6 h. The red solid formed was filtered off, washed twice with diethyl ether and with acetone–diethyl ether (1:4) until the washing liquids were colourless. Yield: 30% for both complexes.

(2) To an acetone solution (15 cm^3) of $[Ru(dps)_2(pyz)X][PF_6]$ (0.5 mmol) was added the solvent species $[Ru(dps)_2(solv)X][PF_6]$ (0.5 mmol) obtained as described in route (1). The time of reaction, all the manipulations and yields were the same.

Complex **7a** (Found: C, 36.85; H, 2.90; N, 9.80; S, 9.00. $C_{44}H_{40}Cl_2F_{12}N_{10}O_2Ru_2S_4$ requires C, 36.90; H, 2.80; N, 9.80; S, 8.95%). IR: 1586s, 1552ms, 1354s, 839 (br), 762s, 737ms, 559vs and 309 ms cm^{-1}. Λ_M(MeCN, 2 × 10^{-4} mol dm^{-3}, 20 °C) = 300 Ω^{-1} mol^{-1}. Complex **7b** (Found: C, 37.70; H, 2.80; N, 11.55; S, 8.85. $C_{45.5}H_{39}F_{12}N_{12}O_{4.5}P_2Ru_2S_4$ requires C, 37.80; H, 2.70; N, 11.60; S, 8.85%). IR: 1712s, 1588s, 1561ms, 1343s, 1292s, 848vs, 772s, 728ms and 559s cm^{-1}. Λ_M(MeCN, 2 × 10^{-4} mol dm^{-3}, 20 °C) = 290 Ω^{-1} cm^2 mol^{-1}.

$[Ru(dps)_2(4,4'\text{-bipy})Cl][PF_6]\cdot H_2O$ **6c**. The complex $[Ru(dps)_2Cl_2]\cdot 2H_2O$ (0.293 g, 0.5 mmol), and $AgPF_6$ (0.126 g, 0.5 mmol) were mixed in acetone (25 cm^3), protected from light and stirred under N_2. After 1 h 4,4′-bipyridine (0.469 g, 3.0 mmol) was added and the mixture was allowed to stir for 3 h. Then it was concentrated, adsorbed onto alumina and added to the top of a 20 × 1 cm diameter chromatography column (Aldrich; aluminium oxide, activated, neutral, STD grade, 150 mesh). Elution with acetone–toluene (4:1) gave an orange band which was collected, concentrated and treated with diethyl ether. The orange solid obtained was crystallized. Yield *ca.* 60% (Found: C, 43.30; H, 3.20; N, 10.10; S, 7.60. $C_{30}H_{26}ClF_6N_6OPRuS_2$ requires C, 43.30; H, 3.15; N, 10.10; S, 7.70%). IR: 1615s, 1595s, 1557ms, 1530ms, 842vs, 771s, 560vs and 327ms cm^{-1}. Λ_M(MeCN, 2 × 10^{-4} mol dm^{-3}, 20 °C) = 161 Ω^{-1} cm^2 mol^{-1}.

Complex **6a** was obtained in the same way starting from $[Ru(dps)_2Cl_2]\cdot 2H_2O$ (0.293 g, 0.5 mmol), $AgPF_6$ (0.126 g, 0.5 mmol) and pyrazine (0.24 g, 3 mmol). The reaction mixture obtained was purified by chromatography using methanol–toluene (2:1) as eluent and crystallized. Yield *ca.* 65%.

$[Ru(dps)_2(py)Cl][PF_6]\cdot 0.5Me_2CO$ **6d**. This complex was obtained in the same way as that of **6c** by starting from $[Ru(dps)_2Cl_2]\cdot 2H_2O$ (0.293 g, 0.5 mmol), $AgPF_6$ (0.126 g, 0.5 mmol) and pyridine (py) (0.237 g, 3 mmol). The reaction mixture obtained was purified by chromatography using toluene–acetone (5:2) as eluent and crystallized. Yield *ca.* 60% (Found: C, 41.50; H, 3.15; N, 9.10; S, 8.40. $C_{26.5}H_{24}ClF_6N_5O_{0.5}PRuS_2$ requires C, 41.55; H, 3.15; N, 9.15; S, 8.35%). IR: 1710s, 1602ms, 1583s, 1551ms, 1530ms, 838vs, 780s, 762s, 727ms, 714ms, 705ms, 558vs and 305ms cm^{-1}. Λ_M(MeCN, 2 × 10^{-4} mol dm^{-3}, 20 °C) = 161 Ω^{-1} cm^2 mol^{-1}.

$[\{Ru(dps)_2Cl\}_2(\mu\text{-}4,4'\text{-bipy})][PF_6]_2\cdot H_2O$ **7c**. The complex $[Ru(dps)_2Cl_2]\cdot 2H_2O$ (0.293 g, 0.5 mmol) and $AgPF_6$ (0.126 g, 0.5 mmol) were mixed in acetone (20 cm^3), protected from light and stirred under N_2. After 1 h 4,4′-bipyridine (0.80 g, 0.51 mmol) was added and the mixture allowed to stir overnight. Then it was adsorbed onto alumina and added to the top of a 20 × 1 cm diameter column (Aldrich; aluminium oxide, activated, neutral, STD grade, 150 mesh) and eluted with acetone. The red-orange band (constantly protected from light) was collected, concentrated and precipitated with diethyl ether. The resulting red solid was washed with diethyl ether–acetone (4:1) until the washings were colourless. The final yield was *ca.* 50% (Found: C, 40.20; H, 2.90; N, 9.35; S, 8.65. $C_{50}H_{42}Cl_2F_{12}N_{10}OP_2Ru_2S_4$ requires C, 40.30; H, 2.85; N, 9.40; S, 8.60%). IR: 1613s, 1586ms, 1552ms, 841vs, 767s, 725ms and 559vs cm^{-1}. Λ_M(MeCN, 2 × 10^{-4} mol dm^{-3}, 20 °C) = 305 Ω^{-1} cm^2 mol^{-1}.

Complex **7a** was obtained in exactly the same way starting from $[Ru(dps)_2Cl_2]\cdot 2H_2O$ (0.293 g, 0.5 mmol), $AgPF_6$ (0.126 g, 0.5 mmol) and pyrazine (0.024 g, 0.3 mmol). Yield *ca.* 50%.

$[Ru(dps)_2Cl_2][PF_6]$ **8**. To a stirred acetone (15 cm^3) suspension of $[Ru(dps)_2Cl_2]\cdot 2H_2O$ (0.293 g, 0.5 mmol) was added dropwise a concentrated solution of HNO_3 until the solid was dissolved [a solution of cerium(IV) salts in the presence of HCl can be also used]. The solution was filtered and added to an aqueous solution of NH_4PF_6. The brown solid obtained was filtered off and washed with water. Yield: 0.28 g (80%) (Found: C, 34.55; H, 2.30: N, 8.05; S, 9.25. $C_{20}H_{16}Cl_2F_6N_4PRuS_2$ requires C, 34.65; H, 2.35; N, 8.10; S, 9.25%). IR: 1591s, 1587s, 1560ms, 1545s, 898s, 834vs, 772vs, 739ms, 558vs, 529s, 357ms, 322s and 309ms cm^{-1}. Λ_M(MeCN, 2 × 10^{-4} mol dm^{-3}, 20 °C) = 160 Ω^{-1} cm^2 mol^{-1}.

Crystal Structure Determination of $[Ru(dps)_2Cl_2]$ **1a**.—Suitable crystals of complex **1a** were obtained by slow evaporation of the solvent from an acetonitrile solution. Single-crystal X-ray diffraction measurements were performed at room temperature on a Siemens R3m/v automatic four-circle diffractometer using graphite-monochromatized Mo-Kα radiation.

The cell parameters were obtained by least-squares fit of 32 accurately centred reflections with 2θ 15–30°, found by a random search of the reciprocal lattice. 3179 Reflections were collected by the variable-speed ω–2θ scan method up to 2θ 52° (h −1 to 10, k −20 to 3, l −1 to 18). The intensities of three standard reflections, monitored after every 197 measurements, remained unchanged with only statistical fluctuations. The intensities were evaluated by the learnt-profile procedure[13] and then corrected for Lorentz and polarization effects. A semiempirical absorption correction was applied (transmission range 0.305–0.337 mm^{-1}) by least-squares fitting a pseudo-ellipsoid to the azimuthal scan data of 12 suitable reflections with high χ angles.[14] From the 2102 unique reflections (R_{int} = 0.006), 1271 were considered observed [$F_o \geqslant 5\sigma(F_o)$] for the refinement of the structure model.

Crystal data. $C_{20}H_{16}N_4RuS_2$, M = 548.5, orthorhombic, space group *Pbcn* (ITC no. 60), a = 8.587(2), b = 16.421(3), c = 15.023(3) Å, U = 2118.5(6) Å^3, Z = 4, D_c = 1.720 g cm^{-3}, F(000) = 1096, μ(Mo-Kα) = 12.04 cm^{-1}, λ(Mo-Kα) = 0.710 73 Å.

The structure was solved by standard Patterson methods and subsequently completed by a combination of least-squares techniques and Fourier syntheses. All non-hydrogen atoms were refined anisotropically. All the hydrogen atoms were located on the last Fourier-difference maps and then included in the refinement with individual isotropic thermal parameters.

The structure model was refined by full-matrix least squares minimizing the function $\Sigma w(F_o - F_c)^2$, converging to $R = \Sigma|F_o - F_c|/\Sigma F_o$ = 0.024 and $R' = \Sigma w^{\frac{1}{2}}|F_o - F_c|/\Sigma w^{\frac{1}{2}}F_o$ = 0.029 with the final weighting scheme $w = [\sigma^2(F_o) + 0.0009F_o^2]^{-1}$. The last difference map showed no significant electron-density residuals, all less than 0.3 e Å^{-3}. Neutral-atom scattering factors and anomalous dispersion corrections were taken into account.[15] Final atomic coordinates for the non-hydrogen atoms are given in Table 1.

Data reduction, structure solution and refinement and drawings were performed with the SHELXTL PLUS package,[16] while final geometrical calculations were carried out with the PARST program,[17] on a DEC MicroVax/3400 computer.

Table 1 Fractional atomic coordinates for the non-hydrogen atoms with estimated standard deviations (e.s.d.s) in parentheses for complex **1a**

Atom	*X/a*	*Y/b*	*Z/c*
Ru	0	0.043 77(2)	0.25
S	0.237 4(2)	0.203 67(7)	0.301 15(8)
Cl	−0.096 7(1)	−0.057 36(6)	0.353 21(8)
C(1)	0.306 1(5)	0.105 1(3)	0.327 3(3)
N(2)	0.216 7(3)	0.039 8(2)	0.311 7(2)
C(3)	0.276 7(6)	−0.034 0(3)	0.332 9(3)
C(4)	0.423 9(7)	−0.042 4(5)	0.370 0(4)
C(5)	0.513 0(7)	0.025 1(5)	0.386 3(4)
C(6)	0.454 3(5)	0.098 5(5)	0.365 0(4)
C(7)	0.177 7(5)	0.193 4(2)	0.188 8(3)
N(8)	0.088 4(3)	0.129 7(2)	0.163 1(2)
C(9)	0.055 6(5)	0.125 3(3)	0.075 0(3)
C(10)	0.098 9(6)	0.183 5(3)	0.005 1(3)
C(11)	0.181 0(7)	0.249 7(3)	0.043 9(3)
C(12)	0.223 5(6)	0.253 9(3)	0.031 2(3)

Additional material available from the Cambridge Crystallographic Data Centre comprises H-atom coordinates, thermal parameters and remaining bond lengths and angles.

Results and Discussion

The reaction of $RuCl_3$ with dps in dmf gave complex **1a** as a red solid. Work-up of the mother-liquors (see Experimental section) allowed the isolation of $[Ru(dps)(dmf)(CO)Cl_2]$ **2** and $[Ru(dps)_2(CO)Cl][PF_6]$ **3**. Similar carbonylated compounds have been reported.[1b,4]

The pyrazine derivatives of complex **1a** have been obtained, according to literature data,[8a,b,10] by routes involving the formation of nitrosyl compounds. These react with stoichiometric amounts of pyz giving the binuclear compounds $[\{Ru(dps)_2X\}_2(\mu\text{-pyz})][PF_6]_2$ (X = Cl **7a** or NO_2 **7b**) while with a large excess of pyz they lead to the formation of mononuclear species (**6a** and **6b**). Complexes **7a** and **7b** may be also obtained by reacting **6a** and **6b** with the solvent species. These routes are lengthy and the yields are very low. Furthermore attempts to prepare the pyridine (py) and 4,4′-bipyridine derivatives from the nitrosyl compounds failed. On the other hand the compound $[Ru(dps)_2(MeCN)_2][PF_6]_2$ **1c** was readily prepared by reaction of **1a** with $AgPF_6$ (ratio 1 : 2) in MeCN, but all attempts to substitute acetonitrile with other ligands like bipy, dps, pyz or 4,4′-bipy failed to give any reaction. Also treatment of **1a** in the same solvent with pyz or 4,4′-bipy in the presence of Ag^+ (ratio 1 : 1) was also unsuccessful. The results suggested the use of a more substitution-labile solvent species. Although attempts to isolate the bis(acetone) complex failed we thought that it would be easy to replace acetone with other ligands *in situ*. As shown in Scheme 1, **6a** and **6c** were obtained easily and with higher yields by treating **1a** dissolved in acetone with $AgPF_6$ (ratio 1 : 1) and a large excess of the dibasic compound. Complex $[Ru(dps)_2(py)Cl][PF_6]$ **6d** was obtained similarly. The same reaction performed with the stoichiometric amount of pyz and 4,4′-bipy gave **7a** and **7c**. Further information on this method is provided in the Experimental section.

The neutral compounds **1a** and **1b** are red and orange solids respectively, slightly soluble in acetonitrile and dimethyl sulfoxide, while the mononuclear ionic compounds are orange solids moderately soluble in acetone and acetonitrile. All the mononuclear compounds are stable for some months in the solid state and some days in solution, whereas the binuclear compounds **7a**–**7c** are red solids moderately soluble in acetonitrile in which they are stable for *ca.* 20 min. The molar conductances of the ionic compounds are in the expected range (see Experimental section).

Crystal Structure of Complex **1a**.—The ruthenium atom occupies a special position on a crystallographic two-fold axis which forces the mononuclear complex to assume a perfect C_{2v} arrangement. The asymmetric unit of the cell contains only half of the molecule (Fig. 1) with only one Cl atom and one dps ligand independent.

The two dps ligands, chelated *via* the N atoms, and the two chlorine atoms, in *cis* position, form an almost ideal octahedral

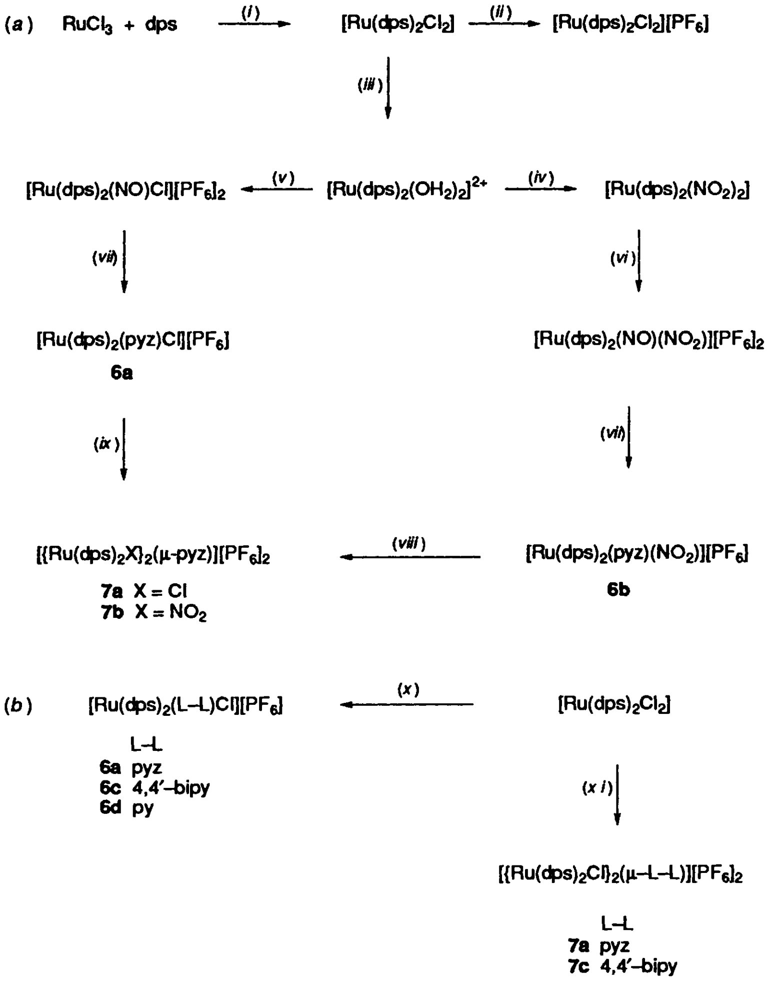

Scheme 1 Synthetic pathways for the preparation of the complexes: (*a*) through nitrosyl derivatives; (*b*) direct method. (*i*) dmf; (*ii*) HNO_3, NH_4PF_6; (*iii*) water; (*iv*) $NaNO_2$; (*v*) HCl, $NaNO_2$, NH_4PF_6; (*vi*) HPF_6; (*vii*) N_3^-, pyz (excess); (*viii*) $[Ru(dps)_2(solv)(NO_2)][PF_6]$; (*ix*) $[Ru(dps)_2(solv)Cl][PF_6]$; (*x*) Me_2CO, $AgPF_6$, L–L (excess); (*xi*) Me_2CO, $AgPF_6$, L–L

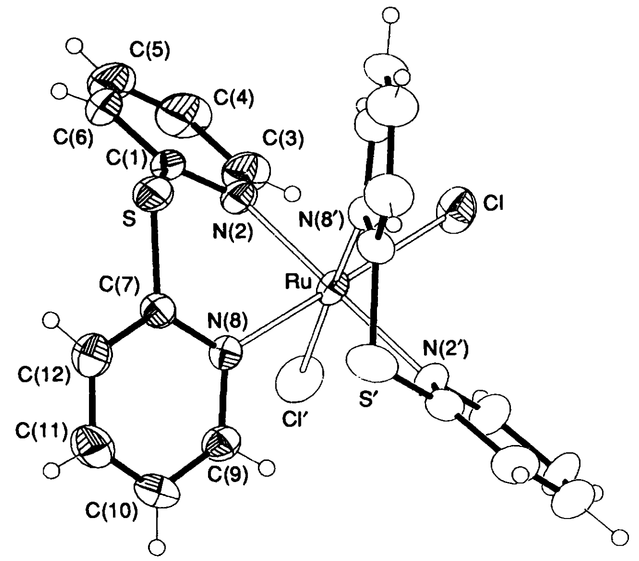

Fig. 1 View of the molecular unit showing the numbering scheme. Thermal ellipsoids are drawn at the 40% probability level, while hydrogen atom size is arbitrary. Dashed thermal ellipsoids represent the atoms of the asymmetric unit while the other half-molecule is obtained by the symmetry operation $-x, +y, -z + \frac{1}{2}$

Table 2 Selected bond lengths (Å) and angles (°) with e.s.d.s in parentheses for complex **1a**. The primes denote the corresponding positions related by the symmetry operation $-x, +y, -z + \frac{1}{2}$ of the crystallographic two-fold axis

Ru–Cl	2.419(1)		
Ru–N(2)	2.079(3)	Ru–N(8)	2.066(3)
S–C(1)	1.767(5)	S–C(7)	1.772(4)
C(1)–N(2)	1.339(5)	C(7)–N(8)	1.353(5)
N(2)–C(3)	1.355(6)	N(8)–C(9)	1.355(5)
C(3)–C(4)	1.388(8)	C(9)–C(10)	1.364(6)
C(4)–C(5)	1.37(1)	C(10)–C(11)	1.366(7)
C(5)–C(6)	1.35(1)	C(11)–C(12)	1.363(7)
C(1)–C(6)	1.397(6)	C(7)–C(12)	1.375(6)
N(2)–Ru–N(2')	176.4(1)	N(8)–Ru–N(8')	93.9(1)
N(2)–Ru–N(8)	88.5(1)	N(2')–Ru–N(8)	93.9(1)
Cl'–Ru–N(2)	87.53(9)	Cl–Ru–N(8')	86.44(9)
Cl–Ru–N(8)	178.52(9)	Cl–Ru–N(2)	90.03(9)
Cl–Ru–Cl'	93.30(4)	C(1)–S–C(7)	102.8(2)
S–C(1)–C(6)	117.8(4)	S–C(7)–C(12)	116.6(3)
S–C(1)–N(2)	120.2(3)	S–C(7)–N(8)	120.6(3)
C(1)–N(2)–C(3)	117.2(3)	C(7)–N(8)–C(9)	115.9(3)

co-ordination sphere about the ruthenium atom as evidenced by the bond angles (Table 2) and by the perfect orthogonality of the three mean co-ordination planes through the Ru atom. The distortion from the ideal arrangement is mainly due to the obviously different lengths of the two Ru–Cl and the four Ru–N bonds. The bite of the chelating dps is large enough [N ••• N = 2.89(1) Å] to allow a value for the corresponding N–Ru–N angle [88.5(1)°] only slightly less than the expected 90° and very close to those found in the analogous complexes [Pd(dps)-Cl_2][11b] and [Pd(η^3-CH_2CHCH_2)(dps)][Pd(η^3-CH_2CHCH_2)-Cl_2].[11c] This value is further favoured by the stable boat conformation of the six-membered ring Ru–N(2)–C(1)–S–C(7)–N(8). The puckering coordinates[18] [θ = 92.2(2), φ = 117.4(2)° and Q = 0.892(2)] of the six-membered ring indicates an almost perfect 'boat' arrangement (quite flat) with the S and Ru atoms about 0.77 Å from the mean plane through the other four ring atoms, on the same side. The boat conformation of this ring is determined by the direction of the two nitrogen lone pairs pointing out on the same side as the sulfur, toward the metal centre. This arrangement is due to the reciprocally rotated disposition of the two pyridines [57.5(1)°]. The twisted N,N-inside conformation of the ligand corresponds to the best pyridine dihedral angle for chelation of the metal, whereas the bite size of the known unco-ordinated dps derivatives appears too small (mean N ••• N 2.62 Å) where the pyridine rings are almost coplanar[19] or too large (3.15 Å) where the disposition is orthogonal.[20] Chelation becomes impossible for bigger rotations[21] where the pyridine nitrogens are *trans* (N ••• N > 4.5 Å). The chelating action of dps in the present compound is favoured by the combination of the boat conformations of the two six-membered rings and the twisted N,N-inside conformations of the two dps ligands, in agreement with models and the reported structures of the palladium complexes.[11b,c]

A remarkable feature of this structure is its similarity to that of [Ru(bipy)$_2$Cl$_2$][22] and other Ru^{II}(bipy) complexes. The length of the Ru–Cl bonds determined here [2.419(1) Å] does not differ significantly from that in the above cited compound [2.426(1) Å]. The mean of the Ru–N bond lengths is quite comparable to the values found in [Ru(bipy)$_3$][PF$_6$]$_2$[23] [2.056(6) Å] or [Ru(bipy)$_2$(MeCN)$_2$][PF$_6$]$_2$[24] [mean 2.054(6) Å]. The Ru–N(2) bond length, *trans* to the equivalent N(2') nitrogen, 2.079(3) Å is slightly larger than that [2.066(3) Å] of Ru–N(8) *trans* to the chlorine atom, as observed in [Ru(bipy)$_2$Cl$_2$] [2.054(2) and 2.013(2) Å, respectively] and in [Ru(bipy)$_2$(CO)Cl][ClO$_4$][25] [means 2.10(2) and 2.07(1) Å, respectively].

Spectroscopic Properties.—The IR spectra of the compounds (characteristic data are shown in the Experimental section) indicate the presence of the various ligands. For all the complexes synthesized strong bands in the ranges 1595–1560 and 790–760 cm^{-1} are assigned to the dps ligand.[11] For the chloride-containing complexes the ν(Ru–Cl) frequencies are found in the range 295–330 cm^{-1}. In particular two medium-strong bands are observed for **1a** at 303 and 297 cm^{-1}, for **2** at 306 and 296 cm^{-1} and for **8** at 322 and 309 cm^{-1}. The spectra of the two carbonylated compounds **2** and **3** contain very strong bands at 1943 and 1972 cm^{-1}, respectively. In the spectrum of **1c** broad bands in the range 2060–2020 cm^{-1} are characteristic of bound MeCN groups. Very strong bands in the spectra of **5a** and **5b** at 1921 and 1932 cm^{-1}, respectively, are assigned to ν(NO).

The ^{1}H NMR spectrum of [Ru(dps)(dmf)(CO)Cl$_2$] shows, in the pyridine region, the presence of one ABMX system[11] in agreement with the *trans* position of the pyridine rings with respect to the Cl$^-$, whereas the spectra of **1a**–**1c** appear as two ABMX systems and show clearly that in solution the molecular symmetry is C_2 (*trans* isomers should show a single ABMX system). In such an arrangement the two pyridyl rings of each dps ligand are not equivalent. On the other hand, each pyridyl group of a dps ligand is transformed into its homologue in the other dps by rotation about the C_2 axis passing through the Ru atom.

In comparing the pyridine region of the ^{1}H NMR spectrum of complex **1a** with those of **1b** and **1c** we notice not only the presence of two ABMX systems and a relatively large difference between the *o*-protons H^6 (of the pyridine rings opposite each other) and H$^{6'}$ (of the pyridine rings *trans* to the ancillary ligands), but also an increase in the chemical shifts of the H$^{6'}$ protons from **1a** to **1c**. The chemical shift differences between the H^6 and H$^{6'}$ are mainly due to the ring-current effect. The H$^{6'}$ protons are shielded by two pyridine rings, H^6 by one. We apply the same considerations to H^5 and H$^{5'}$ where the differences are smaller (δ 0.4). However the chemical shifts of H$^{6'}$ in **1a**, **1b** and **1c** (in dimethyl sulfoxide, δ 7.82, 8.06 and 8.19, respectively) indicate a small degree of deshielding due probably to an electronic effect. The changes in chemical shift are in qualitative agreement with those of the metal-to-ligand charge transfer (m.l.c.t.) band energies observed in the electronic absorption spectra. Taking also into account the structure of **1a** (where the

Ru–N bond distances *trans* to the Cl groups are slightly shorter than those *trans* to equivalent pyridine nitrogens) we suggest that the deshielding from **1a** to **1c** is due to the reduction in back bonding between the filled d_π orbitals of the metal and the delocalized π^* orbitals of dps by a competitor (NO_2 or MeCN) which has a bigger acceptor character than that of Cl and in **1c** also by the charge of the compound. Similarly the comparison of the chemical shift of the dps *o*-protons of **4** (δ 8.90 in acetone) with that of the $H^{6'}$ protons of **1c** (δ 8.45 in acetone) confirms the strong π-acceptor character of bipy.

Although all the NMR spectra are in agreement with the *cis* configuration the presence of different ancillary ligands in complexes **5a**, **5b** and **6a**–**6d** destroys the C_2 symmetry axis; each pyridyl ring becomes different from the others and shows an ABMX system in the ^1H NMR spectrum and five carbon signals in the ^{13}C NMR spectrum. Despite the complexity of the ^1H NMR spectra of **6a**–**6c** (in addition to four ABMX systems, an AA′XX′ system is present in **6a**, an AA′BB′ system in **6b** and two AA′XX′ systems in **6c**) almost complete assignments were made by employment of two-dimensional techniques.

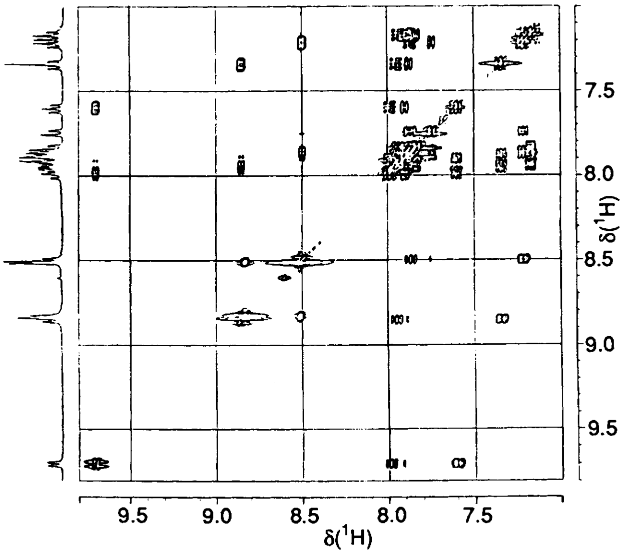

Fig. 2 The COSY ^1H NMR spectrum in $(CD_3)_2CO$ solution of $[Ru(dps)_2(pyz)Cl][PF_6]$ **6a**

The correlation (COSY) spectrum of complex **6a** (Fig. 2) shows that the signals at δ 9.71 (H^{6a}) (Table 3) are correlated to those at δ 7.99 (H^{4a}), 7.91 (H^{3a}) and 7.59 (H^{5a}). We assign these to the protons of the pyridine ring next to the pyrazine group. Similarly the signals at δ 8.85 (H^{6b}), 7.95 (H^{4b}), 7.89 (H^{3b}) and 7.33 (H^{5b}) are assigned to the ring next to the Cl group and those at δ 8.49 ($H^{6a'}$), 7.87 ($H^{4a'}$), 7.74 ($H^{3a'}$) and 7.21 ($H^{5a'}$) to the ring *trans* to the pyrazine group. The $H^{6b'}$ proton *trans* to the Cl group are strongly shielded (δ 7.88) and correlated to the signals at δ 7.93 ($H^{4b'}$), 7.83 ($H^{3b'}$) and 7.16 ($H^{5b'}$). Although the pyrazine signals at δ 8.82 and 8.50 are somewhat overlapped with the H^{6b} and $H^{6a'}$ signals, respectively, and do not allow measurements of coupling constants, they appear as an AA′XX′ system.

On comparing the ^1H NMR spectra of complexes **5a**, **5b** and **6a**–**6d** we observe (Fig. 3) that the *o*-protons H^6 of the pyridine rings opposite each other show nearly the same chemical shift when are next to the same ligand, whereas the $H^{6'}$ resonances are shifted to higher frequencies when the monodentate nitrogen ligands are *trans*.

The ^{13}C NMR data are listed in Table 4. In the spectra of the mononuclear pyrazine, 4,4′-bipyridine and pyridine compounds the C^6, C^4, C^3 and C^5 carbon signals of dps are in the ranges δ 159.5–157.5, 140.0–137.9, 130.0–127.3 and 126.7–124.4, respectively. In the spectra of **6a** and **6b** the pyrazine carbons next to the nitrogen atom bonded to the ruthenium appear deshielded (δ 152.03 and 152.02, respectively) with respect the other carbons (δ 146.91 and 147.11, respectively). For **6c** the 4,4′-bipy carbon signals are observed at δ 157.50, 151.93, 123.51 an 121.91 while for **6d** the pyridine carbons appear at δ 156.54, 137.85 and 126.34 in agreement with rapid rotation of pyz, 4,4′-bipy or py around the Ru–N bond.

The UV/VIS absorption maxima of the complexes are shown in Table 5. The spectra of $[Ru(dps)_2Cl_2]$ and $[Ru(dps)_2Cl_2]PF_6$ contain intense absorptions in the range 290–270 nm assigned as $\pi \longrightarrow \pi^*$ ligand transitions. Lower-energy bands at 458 nm for $[Ru(dps)_2Cl_2]$ and at 480 and 398 nm for $[Ru(dps)_2$-

Table 3 Proton NMR data ($SiMe_4$ as standard) for ruthenium di-2-pyridyl sulfide complexes[a]

Complex	Solvent	H^6	$H^{6'}$	H^4		H^3		H^5	
1a	$(CD_3)_2SO$	9.57	7.82	7.37	7.14	7.25	7.06	6.99	6.55
1b	$(CD_3)_2SO$	9.84[b]	8.06[b]	7.94	7.80	7.79[b]	7.67[b]	7.59	7.19
1c	$(CD_3)_2SO$	9.32[b]	8.19[b]	8.12	7.99	7.95[b]	7.83[b]	7.74	7.32
	$(CD_3)_2CO$	9.59	8.45	8.15	8.00[c]	8.00[c]	7.86	7.75	7.35
4	$(CD_3)_2CO$	8.90		8.32		7.99[c]		7.27	
		7.99[c,d]		8.11[d]	7.96[d]	8.80[d]	8.71[d]	7.74[d]	7.49[d]
5a	$(CD_3)_2CO$	9.22	8.30	8.46[c]	8.44	8.59	8.52	7.90	7.61
		8.71	8.13		8.43	8.51	8.33	7.88	7.52
5b	$(CD_3)_2CO$	9.36	8.27[c]	8.53[c]	8.51	8.59	8.57	7.99	7.59
		9.13			8.41	8.53[c]		7.87	7.57
6a	$(CD_3)_2CO$	9.71	8.49	7.99	7.87	7.91	7.74	7.59	7.21
		8.85	7.88	7.95	7.93	7.89	7.83	7.33	7.16
		8.82[e]	8.50[e]						
6b	$(CD_3)_2CO$	9.60	8.35	7.97[c]	7.90[c]	7.88[c]		7.61	7.24
		9.10	7.81	8.55[f]			7.78	7.44	7.21
6c	$(CD_3)_2CO$	9.78	8.54	7.98[c]	7.95[c]	7.91	7.78[g]	7.62	7.23
		8.94	7.85	8.84[g]	8.72[g]	7.86[g]	7.75	7.31	7.19
6d	$(CD_3)_2CO$	9.76	8.53	7.90[c]		7.81[c]	7.71	7.60	7.18
		8.89	7.85	8.68[h]	7.94[h]	7.41[h]		7.29	7.16
7a	CD_3CN	9.44	8.37	7.89[c]	7.73[c]	7.59	7.41	7.25	7.09[c]
		8.77	7.41	8.30[e]		7.22	7.17		6.89

[a] Recorded at 300 MHz and 298 K. The dps proton signals generally appear as a doublet of doublet of doublets with coupling constants $J(H^5H^6)$ = 6.2–5.8, $J(H^4H^6)$ = 1.3–1.7, $J(H^3H^6)$ = 0.7, $J(H^4H^5)$ = 7.5–7.8, $J(H^3H^5)$ = 1.5–1.8 and $J(H^3H^4)$ = 7.8–8.0 Hz. The pyrazine and 4,4′-bipyridine proton signals appear as AA′XX′ systems unless stated otherwise. [b] $J(H^3H^6)$ not observed. [c] Overlapped signal. [d] 2,2′-Bipyridine signal. The H^3 signals appear as a doublet (J = 8.2). [e] Pyrazine signal. [f] Pyrazine signal as unresolved AA′BB′ system. [g] 4,4′-Bipyridine signal. [h] Broad signal of pyridine.

Table 4 Selected ^{13}C NMR data[a] (SiMe$_4$ as standard) for ruthenium di-2-pyridyl sulfide complexes

Complex	C^6		C^2		C^4		C^3		C^5	
1c	159.50	157.46	156.90	156.85	140.21	139.78	130.18	129.25	126.48	126.30
							128.73[b]		4.25[b]	
	[c] 159.04	157.09	156.78	156.66	139.83	139.34	130.04	129.07	126.01	125.90
							127.95[b]			
4	155.80				139.64		129.54		126.29	
	155.65[d]	152.94[d]	158.87[d]	158.59[d]	139.30[d]	138.88[d]	125.51[d]	125.33[d]	128.54[d]	127.90[d]
5a	156.43	156.02			145.07	144.92	132.18	131.72	129.15	128.44
	155.42	154.97			144.55	143.85	130.75[e]		128.30	127.45
5b	157.09	156.03	156.38	155.07	145.76	144.78	132.40	132.22	128.90	128.46
	155.98	155.48			144.55	144.49	131.99	131.42	128.26	127.73
6a	159.20	159.05	158.16	157.62	138.95	138.80	129.95	128.64	126.71	125.46
	158.82	158.00	152.03[f]	146.91[f]	138.35	138.27	128.13	127.54	124.89	124.60
6b	159.18	158.24	157.40	157.11	147.11[f]	139.88	129.89	129.58	126.58	125.57
	158.12	157.50	156.25	152.02[f]	139.49[e]	139.18	128.20	127.76	125.10	125.04
6c	159.48	159.44	157.50[g]	151.93[g]	138.75	138.70	129.96	128.57	126.62	125.27
	159.29	158.35	123.51[g]	121.91[g]	138.14	138.08	128.16	127.49	124.89	124.59
6d	159.47	159.31	156.54[h]	137.85[h]	138.52	138.50	129.79	128.40	126.39	124.99
	159.19	158.30	126.34[h]		137.94	137.90	128.00	127.31	124.71	124.41

[a] Recorded at 75.56 MHz and 298 K in (CD$_3$)$_2$CO unless stated otherwise. [b] Signals of MeCN. [c] In CD$_3$CN. [d] 2,2′-Bipyridine signal. [e] Overlapped signal. [f] Pyrazine signals. [g] 4,4′-Bipyridine signal. [h] Pyridine signal.

Table 5 The UV/VIS data for ruthenium di-2-pyridyl sulfide complexes in MeCN

Compound	λ_{max}/nm (10^{-3} ε/dm^3 mol^{-1} cm^{-1})
[Ru(dps)$_2$Cl$_2$]	458 (5.4), 392 (sh), 290 (11.0), 280 (sh)
[Ru(dps)$_2$(NO$_2$)$_2$]	388 (2.9), 284 (13.0), 278 (sh)
[Ru(dps)$_2$(MeCN)$_2$][PF$_6$]$_2$	359 (10.5), 290 (sh), 271 (26.0)
[Ru(dps)$_2$(dmf)(CO)Cl$_2$]	390 (2.8), 290 (13.0)
[Ru(dps)$_2$(CO)Cl][PF$_6$]	365 (sh), 280 (23.0)
[Ru(bipy)$_2$(dps)][PF$_6$]$_2$	444 (10.5), 428 (sh), 354 (8.4), 285 (66.5)
[Ru(dps)$_2$(NO)Cl][PF$_6$]$_2$	376 (2.8), 292 (14.5)
[Ru(dps)$_2$(NO)(NO$_2$)][PF$_6$]$_2$	372 (4.6), 288 (sh), 276 (17.5)
[Ru(dps)$_2$(pyz)Cl][PF$_6$]	409 (9.7), 290 (sh), 277 (21.0)
[Ru(dps)$_2$(pyz)(NO$_2$)][PF$_6$]	378 (12.0), 284 (sh), 275 (24.5)
[Ru(dps)$_2$(4,4′-bipy)Cl][PF$_6$]	413 (17.0), 288 (35.0), 278 (sh), 244 (32.0)
[Ru(dps)$_2$(py)Cl][PF$_6$]	413 (11.5), 380 (sh), 290 (25.0), 280 (sh), 244 (14.0)
[{Ru(dps)$_2$Cl}$_2$(μ-pyz)][PF$_6$]$_2$	505 (15.0), 402 (19.5), 288 (sh), 277 (43.5)
[{Ru(dps)$_2$(NO$_2$)}$_2$(μ-pyz)][PF$_6$]$_2$	484 (15.5), 378 (22.0), 292 (sh), 274 (40.0)
[{Ru(dps)$_2$Cl}$_2$(μ-4,4′-bipy)][PF$_6$]$_2$	423 (21.0), 288 (sh), 277 (35.0), 242 (28.0)
[Ru(dps)$_2$Cl$_2$][PF$_6$]	580 (0.4), 480 (1.4), 398 (2.0), 274 (22.0)

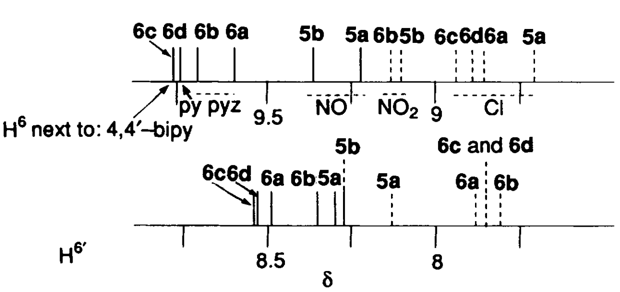

Fig. 3 Schematic presentation of the resonances of the *o*-protons of the pyridine ring opposite each other (top) and opposite to the other ligands (bottom) in complexes **5a**, **5b** and **6a**–**6d**

Cl$_2$][PF$_6$] were assigned as m.l.c.t. and ligand-to-metal charge-transfer (l.m.c.t.)[1b,26] transitions, respectively. In agreement with the m.l.c.t. nature of the band at 458 nm the absorption coefficient is 5.4 × 10^3 dm^3 mol^{-1} cm^{-1}.[1b] The large blue shift (92 nm) of the m.l.c.t. band with respect to that of the corresponding bipyridine complex[1b] suggests dps is a weaker π-acceptor ligand than is bipy. Consistent with this suggestion is the spectrum of [Ru(bipy)$_2$(dps)][PF$_6$]$_2$ in which the lower-energy absorption is split into two bands, one at 444 nm with a shoulder at about 428 nm and another at 354 nm. The longer-wavelength band resembles the peak and shoulder of [Ru(bipy)$_3$]$^{2+}$ and can be assigned to the m.l.c.t. transition involving the bipy ligand. The shorter-wavelength band is assigned to the m.l.c.t. transition involving the dps ligand. The energy of the m.l.c.t. band in the dps compounds is dependent on the nature of the ancillary ligands. Blue shifts are observed on replacing Cl$^-$ by stronger π-acceptor ligands {70 nm for [Ru(dps)$_2$(NO$_2$)$_2$], 99 nm for [Ru(dps)$_2$(MeCN)$_2$][PF$_6$]$_2$, 104 nm for [Ru(bipy)$_2$(dps)][PF$_6$]$_2$}. Blue shifts are also observed for the nitrosyl compounds [Ru(dps)$_2$(NO)X][PF$_6$]$_2$, X = Cl (82) or NO$_2$ (86 nm). Although the mononuclear complexes **6a**–**6d**, and the binuclear complexes **7a**–**7c** should exhibit two $d_\pi(Ru) \longrightarrow \pi^*$ absorptions due to the presence of dps and the monodentate or bridging nitrogen ligands (pyz, 4,4′-bipy and py), only one m.l.c.t. band is observed for **6a**–**6c** and **7c**. For **6d** a band at 413 nm with a shoulder at *ca.* 380 nm is observed. These data are explained in terms of overlapping of the two $d_\pi(Ru) \longrightarrow \pi^*$ absorptions and, according to this suggestion, for binuclear complex **7a** and **7b** two bands are observed. The lowest-energy bands (at 505 and 484 nm, respectively) assigned as $d_\pi(Ru) \longrightarrow \pi^*(pyz)$[27] transitions are red shifted with respect to those of the mononuclear complexes as a result of the stabilization of the π* level of the bridging ligand due to the positive charge of the second ruthenium centre. The other bands assigned as $d_\pi(Ru) \longrightarrow \pi^*(dps)$ remain nearly constant (at 402 and 378 nm, respectively).

Acknowledgements

We are grateful to the Consiglio Nazionale della Ricerche and Ministero dell'Università e della Ricerca Scientifica e Tecnologica (MURST) of Italy for financial support (40 and 60% funding).

References

1 (*a*) B. P. Sullivan, D. J. Salmon and T. J. Meyer, *Inorg. Chem.*, 1978, **17**, 3334; (*b*) A. Basu, T. G. Kasar and N. Y. Sapre, *Inorg. Chem.*,

1988, **27**, 4539; (*c*) M. Kakoti, A. K. Deb and S. Goswami, *Inorg. Chem.*, 1992, **31**, 1302; (*d*) S. Chirayil and R. P. Thummel, *Inorg. Chem.*, 1988, **28**, 813; (*e*) S. Chirayil, V. Hegde, Y. Jahng and R. P. Thummel, *Inorg. Chem.*, 1991, **30**, 2821; (*f*) M. A. Hayes, C. Meckel, E. Schatz and M. D. Ward, *J. Chem. Soc., Dalton Trans.*, 1992, **703**.

2 D. G. Witten, *Acc. Chem. Res.*, 1980, **13**, 83; K. Kalyanasundaram, *Coord. Chem. Rev.*, 1982, **46**, 159; A. Juris, V. Balzani, F. Barigelletti, S. Campagna, P. Belser and A. Von Zelewsky, *Coord. Chem. Rev.*, 1988, **84**, 85; T. J. Meyer, *Acc. Chem. Res.*, 1989, **22**, 163; *Pure Appl. Chem.*, 1990, **62**, 1003; J. K. Nagle and D. M. Roundhill, *Chemtracts: Inorg. Chem.*, 1992, **4**, 141.

3 S. W. Gersten, G. J. Samuels and T. J. Meyer, *J. Am. Chem. Soc.*, 1982, **104**, 4029; S. Goswami, A. R. Chakravarty and A. Chakravorty, *J. Chem. Soc., Chem. Commun.*, 1982, 1288; T. J. Meyer, *Electrochem. Soc.*, 1984, **131**, 221C; K. Kalyanasunduram, G. Grätzel and E. Pellizzetti, *Coord. Chem. Rev.*, 1986, **69**, 57.

4 J. P. Collin and J. P. Sauvage, *Inorg. Chem.*, 1986, **25**, 135.

5 B. J. Coe, T. J. Meyer and P. S. White, *Inorg. Chem.*, 1993, **32**, 4012.

6 C. A. Bignozzi, C. Chiorboli, Z. Murtaza, E. J. Wayne and T. J. Meyer, *Inorg. Chem.*, 1993, **32**, 1036; T. C. Strekas, H. D. Gafney, S. A. Tysoe, R. T. Thummel and F. Lefoulon, *Inorg. Chem.*, 1989, **28**, 2964.

7 C. H. Braunstein, A. D. Baker, T. C. Strekas and H. D. Gafney, *Inorg. Chem.*, 1984, **23**, 857; D. A. Geselowitz, W. Kutner and T. J. Meyer, *Inorg. Chem.*, 1986, **25**, 2015; W. J. Vining and T. J. Meyer, *Inorg. Chem.*, 1986, **25**, 2023.

8 (*a*) R. W. Callahan, G. M. Brown and T. J. Meyer, *Inorg. Chem.*, 1975, **7**, 1443; (*b*) R. W. Callahan, F. R. Keene, T. J. Meyer and D. J. Salmon, *J. Am. Chem. Soc.*, 1977, **16**, 1064; (*c*) K. A. Goldsby and T. J. Meyer, *Inorg. Chem.*, 1984, **23**, 3002; (*d*) W. Kaim and K. V. Kasac, *Inorg. Chem.*, 1990, **29**, 4696; (*e*) M. Haga and A. M. Bond, *Inorg. Chem.*, 1991, **30**, 475; (*f*) C. A. Bignozzi, R. A. Argazzi, J. R. Schoonover, K. C. Gordon, R. B. Dyer and F. Scandola, *Inorg. Chem.*, 1992, **31**, 5260.

9 G. F. Strouse, P. A. Anderson, J. R. Schoonover, T. J. Meyer and F. R. Keene, *Inorg. Chem.*, 1992, **31**, 3004; D. A. Reitsma and F. R. Keene, *J. Chem. Soc., Dalton Trans.*, 1992, 2859.

10 J. B. Godwin and T. J. Meyer, *Inorg. Chem.*, 1971, **10**, 471; S. A. Adeyemi, J. N. Braddock, G. M. Brown, J. A. Ferguson, F. J. Miller and T. J. Meyer, *J. Am. Chem. Soc.*, 1972, **12**, 300; S. A. Adeyemi, C. E. Johnson, F. J. Miller and T. J. Meyer, *Inorg. Chem.*, 1973, **10**, 2371.

11 (*a*) G. Tresoldi, P. Piraino, E. Rotondo and F. Faraone, *J. Chem. Soc., Dalton Trans.*, 1991, **425**; (*b*) G. Tresoldi, E. Rotondo, P. Piraino, M. Lanfranchi and A. Tiripicchio, *Inorg. Chim. Acta*, 1992, **194**, 233; (*c*) G. De Munno, G. Bruno, E. Rotondo, G. Giodano, S. Lo Schiavo, P. Piraino and G. Tresoldi, *Inorg. Chim. Acta*, 1993, **208**, 67.

12 C. Chachaty, G. C. Pappalardo and G. Scarlata, *J. Chem. Soc., Perkin Trans. 2*, 1976, 1234.

13 R. Diamond, *Acta Crystallogr., Sect. A*, 1969, **27**, 43.

14 G. Kopfmann and R. Hubert, *Acta Crystallogr., Sect. A*, 1968, **24**, 348.

15 J. A. Ibers and W. C. Hamilton, *International Tables for X-Ray Crystallography*, Kynoch Press, Birmingham, 1974, vol. 4.

16 SHELXTL PLUS, version 4.2, Siemens Analytical X-Ray Instruments, Madison, 1991.

17 M. Nardelli, *Comput. Chem.*, 1983, **7**, 95.

18 D. Cremer and J. A. Pople, *J. Am. Chem. Soc.*, 1975, **97**, 1354.

19 G. Bombieri, E. Forsellini and R. Graziani, *Acta Crystallogr., Sect. B*, 1978, **34**, 2622; G. Bombieri, E. Forsellini, R. Graziani and G. C. Pappalardo, *Transition Met. Chem.*, 1979, **4**, 70.

20 M. Kimura, S. H. Simonsen, S. R. Caldwell and G. E. Martin, *J. Heterocycl. Chem.*, 1981, **18**, 469.

21 M. E. Amato, G. Bandoli, A. Grassi, G. C. Pappalardo and G. Scarlata, *Phosphorus, Sulphur, Silicon Relat. Elem.*, 1989, **45**, 197.

22 D. S. Eggleston, K. A. Goldsby, D. J. Hodgson and T. J. Meyer, *Inorg. Chem.*, 1985, **24**, 4573.

23 D. P. Rillema, D. S. Jones and H. A. Levy, *J. Chem. Soc., Chem. Commun.*, 1979, 849.

24 M. J. Heeg, R. Kroener and E. Deutsch, *Acta Crystallogr., Sect. C*, 1985, **41**, 684.

25 J. M. Clear, J. M. Kelly, C. M. O'Connell, J. G. Vos, C. J. Cardin, S. R. Costa and A. J. Edwards, *J. Chem. Soc., Chem. Commun.*, 1980, 750.

26 M. K. Nazeeruddin, S. M. Zakeeruddin and K. Kalyanasundaram, *J. Phys. Chem.*, 1993, **97**, 9607.

27 D. P. Rillema and K. B. Mack, *Inorg. Chem.*, 1982, **21**, 3849.

Received 26*th May* 1994; *Paper* 4/03152K